

# Quantum Random Walks without Coin Toss\*

Apoorva Patel

(Collaborators: K.S. Raghunathan and Pranaw Rungta)

Centre for High Energy Physics,

Indian Institute of Science, Bangalore-560012, India

E-mail: adpatel@cts.iisc.ernet.in

We construct a quantum random walk algorithm, based on the Dirac operator instead of the Laplacian. The algorithm explores multiple evolutionary branches by superposition of states, and does not require the coin toss instruction of classical randomised algorithms. We use this algorithm to search for a marked vertex on a hypercubic lattice in arbitrary dimensions. Our numerical and analytical results match the scaling behaviour of earlier algorithms that use a coin toss instruction.

PACS numbers: 03.67.Lx

## I. INTRODUCTION

Random walks are a fundamental ingredient of non-deterministic algorithms [1], and are used to tackle a wide variety of problems—from graph structures to Monte Carlo samplings. Such algorithms have many evolutionary branches, which are explored probabilistically, to estimate the correct result. A classical computer can explore only one branch at a time, so the algorithm is executed several times, and the estimate of the final result is extracted from the ensemble of individual executions by methods of probability theory. Such algorithms are typically represented using graphs, with vertices denoting the states and the edges denoting the evolutionary routes. A particular evolution corresponds to a specific walk on the graph, and the final result is obtained by combining the results for many different walks. To ensure that different evolutionary branches are explored in different executions, one needs non-deterministic instructions, and they are provided in the form of random numbers. A coin toss is the simplest example of a random number generator, and it is included in the instruction set for a probabilistic Turing machine.

A quantum computer can explore multiple branches of a non-deterministic algorithm in a single attempt, by using a clever superposition of states. The probabilistic result can then be arrived at by interference of amplitudes corresponding to different branches. Thus as long as the means to construct a variety of superposed states exist, there is no a priori reason to include a coin toss as an instruction for a (probabilistic) quantum Turing machine.

In what follows, we construct a quantum random walk on a hypercubic lattice in arbitrary dimensions without using a coin toss instruction, analyse its properties, and use it to find a marked vertex on the lattice. More details are available in Refs.[2, 3].

## II. DIFFUSION

A random walk is a diffusion process, commonly described using the Laplacian operator in the continuum. To construct a discrete quantum random walk, we must discretise the diffusion process using evolution operators that are both unitary and ultra-local (an ultra-local operator vanishes outside a finite range).

On a periodic lattice, the spatial modes are characterised by discrete wave vectors  $\vec{k}$ . Quantum diffusion then depends on the energy of these modes according to  $U(\vec{k}, t) = \exp(-iE(\vec{k})t)$ . The lowest energy mode,  $\vec{k} = 0$ , corresponding to a uniform distribution, is an eigenstate of the diffusion operator and does not propagate. The slowest propagating modes are the ones with smallest nonzero  $|\vec{k}|$ . The classical Laplacian operator gives  $E(\vec{k}) \propto |\vec{k}|^2$  [4], which translates to the characteristic Brownian motion signature, spread  $\langle n \rangle_{\text{rms}} \propto \sqrt{t}$ . There is an alternative in quantum theory—instead of the non-relativistic Schrödinger equation based on the Laplacian operator  $\nabla^2$ , one can use the relativistic Dirac equation based on the operator  $\nabla$ . The Dirac operator gives  $E(\vec{k}) \propto |\vec{k}|$ , with the associated signature, spread  $\langle n \rangle_{\text{rms}} \propto t$ . Clearly the Dirac operator, with its faster diffusion of the slowest modes compared to the Laplacian, is the operator of choice for constructing faster diffusion based quantum algorithms.

An automatic consequence of the Dirac operator is the appearance of an additional internal degree of freedom corresponding to spin, whereby the quantum state is described by a multi-component spinor. These spinor components were identified with the states of a coin in Refs.[5, 6], with the coin evolution rule guiding the quantum diffusion process. While this is the correct procedure in the continuum theory, another option is available for a lattice theory, i.e. staggered fermions [7]. In this approach, the spinor degrees of freedom are spread out over an elementary hypercube, location dependent signs appear in the evolution operator, and translational invariance exists in steps of 2 instead of 1. We follow this approach to construct, a quantum diffusion process on a hypercubic lattice, without a coin toss instruction,

---

\*Invited lecture at the Workshop on Quantum Information, Computation and Communication (QICC-2005), IIT Kharagpur, India, February 2005, quant-ph/0506221.



$$H_o \propto \begin{pmatrix} \cdots & \cdots & \cdots & \cdots & \cdots & \cdots & \cdots & \cdots & \cdots \\ \cdots & 0 & 1 & -1 & 0 & 0 & 0 & \cdots & \\ \cdots & 0 & -1 & 1 & 0 & 0 & 0 & \cdots & \\ \cdots & 0 & 0 & 0 & 1 & -1 & 0 & \cdots & \\ \cdots & 0 & 0 & 0 & -1 & 1 & 0 & \cdots & \\ \cdots & \cdots & \cdots & \cdots & \cdots & \cdots & \cdots & \cdots & \cdots \end{pmatrix}. \quad (12)$$

While  $H$  has the structure of a second derivative, its two parts,  $H_e$  and  $H_o$ , have the structure of a first derivative. The above decomposition is indeed reminiscent of the ‘‘square-root’’ one takes to go from the Laplacian to the Dirac operator.

The two parts,  $H_e$  and  $H_o$ , are individually Hermitian. They are block-diagonal with a constant  $2 \times 2$  matrix, and so they can be exponentiated while maintaining ultra-locality. The total evolution operator can therefore be easily truncated, without giving up either unitarity or ultra-locality,

$$U(\Delta t) = e^{i(H_e + H_o)\Delta t} = e^{iH_e\Delta t} e^{iH_o\Delta t} + O((\Delta t)^2) \quad (13)$$

$$= U_e(\Delta t) U_o(\Delta t) + O((\Delta t)^2).$$

The quantum random walk can now be generated using  $U_e U_o$  as the evolution operator for the amplitude distribution  $\psi(n, t)$ ,

$$\psi(n, t) = [U_e U_o]^t \psi(n, 0), \quad (14)$$

The fact that  $U_e$  and  $U_o$  do not commute with each other is enough for the quantum random walk to explore all possible states. The price paid for the above manipulation is that the evolution operator is translationally invariant along the line in steps of 2, instead of 1.

The  $2 \times 2$  matrix appearing in  $H_e$  and  $H_o$  is proportional to  $(1 - \sigma_1)$ , and so its exponential will be of the form  $(c1 + is\sigma_1)$ ,  $|c|^2 + |s|^2 = 1$ . A random walk should have at least two non-zero entries in each row of the evolution operator. Even though our random walk treats even and odd sites differently by construction, we can obtain an unbiased random walk, by choosing the  $2 \times 2$  blocks of  $U_e$  and  $U_o$  as  $\frac{1}{\sqrt{2}} \begin{pmatrix} 1 & i \\ i & 1 \end{pmatrix}$ . Furthermore, it is computationally more convenient to choose a basis where the unitary operators are all real. Performing a global phase transformation,  $|n\rangle \rightarrow i^n |n\rangle$  [12], the  $2 \times 2$  blocks of  $U_e$  and  $U_o$  become  $\frac{1}{\sqrt{2}}(1 \pm i\sigma_2)$ . The discrete quantum random walk then evolves the amplitude distribution according to

$$U_o |n\rangle = \frac{1}{\sqrt{2}} \left[ |n\rangle - (-1)^n |n + (-1)^n\rangle \right], \quad (15)$$

$$U_e |n\rangle = \frac{1}{\sqrt{2}} \left[ |n\rangle + (-1)^n |n - (-1)^n\rangle \right], \quad (16)$$

$$U_e U_o |n\rangle = \frac{1}{2} \left[ |n-1\rangle + |n\rangle - |n+1\rangle + |n+2(-1)^n\rangle \right]. \quad (17)$$

It is instructive to realise that, with the above choice, the unbiased quantum random walk represents the path integral for a relativistic particle with  $|p| = m$ . Its speed

(in units of speed of light) is then  $|v| = 1/\sqrt{2}$ . The directed walk, with the  $2 \times 2$  block matrix  $U \propto \sigma_2$ , corresponds to  $|v| = 1$ , and the stationary limit  $U = 1$  corresponds to  $v = 0$ .

## B. Analysis

It is straightforward to analyse the properties of the walk in Eq.(17) using the Fourier transform:

$$\tilde{\psi}(k, t) = \sum_n e^{ikn} \psi(n, t), \quad (18)$$

$$\psi(n, t) = \int_{-\pi}^{\pi} \frac{dk}{2\pi} e^{-ikn} \tilde{\psi}(k, t). \quad (19)$$

The evolution of the amplitude distribution in Fourier space is easily obtained by splitting it in to its even and odd parts:

$$\psi \equiv \begin{pmatrix} \psi_e \\ \psi_o \end{pmatrix}, \quad \psi(k, t) = [M(k)]^t \psi(k, 0), \quad (20)$$

$$M(k) = \begin{pmatrix} e^{ik} \cos k & -i \sin k \\ -i \sin k & e^{-ik} \cos k \end{pmatrix}. \quad (21)$$

The unitary matrix  $M$  has the eigenvalues,  $\lambda_{\pm} \equiv e^{\pm i\omega_k}$  (this  $\pm$  sign label continues in all the results that follow),

$$\lambda_{\pm} = \cos^2 k \pm i \sin k \sqrt{1 + \cos^2 k}, \quad \omega_k = \cos^{-1}(\cos^2 k), \quad (22)$$

with the (unnormalised) eigenvectors,

$$e_{\pm} \propto \begin{pmatrix} -\cos k \mp \sqrt{1 + \cos^2 k} \\ 1 \end{pmatrix},$$

$$\propto \begin{pmatrix} 1 \\ \cos k \mp \sqrt{1 + \cos^2 k} \end{pmatrix}. \quad (23)$$

The evolution of amplitude distribution then follows

$$\tilde{\psi}(k, t) = e^{i\omega_k t} \tilde{\psi}_+(k, 0) + e^{-i\omega_k t} \tilde{\psi}_-(k, 0), \quad (24)$$

where  $\tilde{\psi}_{\pm}(k, 0)$  are the projections of the initial amplitude distribution along  $e_{\pm}$ . The amplitude distribution in the position space is given by the inverse Fourier transform of  $\tilde{\psi}(k, t)$ . While we are unable to evaluate it exactly, many properties of the quantum random walk can be extracted numerically as well as by suitable approximations.

A walk starting at the origin satisfies  $\psi_o(n, 0) = \delta_{n,0}$ . This walk is asymmetric because our definitions treat even and odd sites differently. We can construct a symmetric walk, using the initial condition  $\psi_s(n, 0) = (\delta_{n,0} + i\delta_{n,1})/\sqrt{2}$ . The resultant probability distribution is then symmetric under  $n \leftrightarrow (1 - n)$ . (Real and imaginary components of the amplitude distribution evolve

independently because we have chosen the evolution operator to be real.) For both these initial conditions, by construction, the quantum random walk remains within the interval  $[-2t + 1, 2t]$  after  $t$  time steps.

The escape probability of the quantum random walk can be calculated by introducing a fully absorbing wall, say between  $n = 0$  and  $n = -1$ . Mathematically, this absorbing wall amounts to a projection operator for  $n \geq 0$ . The unabsorbed part of the walk is given by

$$\begin{aligned} \psi(n, t+1) &= P_{n \geq 0} U_e U_o \psi(n, t), \\ &= U_e U_o \psi(n, t) - \frac{1}{2} \delta_{n,-1} (\psi(0, t) + \psi(1, t)), \end{aligned} \quad (25)$$

with the absorption probability,

$$P_{\text{abs}}(t) = 1 - \sum_{n \geq 0} |\psi(n, t)|^2. \quad (26)$$

All these variations in initial and boundary conditions are easy to implement numerically, and examples are shown in Fig.2. We have used such simulations to study various properties of the quantum random walk.

For large  $t$ , a good approximation to the probability distributions can be obtained by the stationary phase method [2, 9]. The smoothed probability distribution for the symmetric walk, obtained by replacing the highly oscillatory terms by their mean values, is

$$|\psi_s|_{\text{smooth}}^2 = \frac{4t^2}{\pi \sqrt{4t^2 - 2n^2} (4t^2 - n^2)}. \quad (27)$$

(Here, the  $n \leftrightarrow (1-n)$  symmetry can be restored by replacing  $n$  by  $(n - \frac{1}{2})$ .) As shown in the top part of Fig.2, it represents the average behavior of the distribution very well. Its low order moments are easily calculated to be,

$$\int_{n=-\sqrt{2}t}^{\sqrt{2}t} |\psi_s|_{\text{smooth}}^2 dn = 1, \quad (28)$$

$$\int_{n=-\sqrt{2}t}^{\sqrt{2}t} |n| \cdot |\psi_s|_{\text{smooth}}^2 dn = t, \quad (29)$$

$$\int_{n=-\sqrt{2}t}^{\sqrt{2}t} n^2 |\psi_s|_{\text{smooth}}^2 dn = 2(2 - \sqrt{2})t^2. \quad (30)$$

### C. Results

The following properties of the quantum random walk are easily deduced [2]:

- The probability distribution is double-peaked with maxima approximately at  $\pm\sqrt{2}t$ . The distribution falls off steeply beyond the peaks, while it is rather flat in the region between the peaks. With increasing  $t$ , the peaks become more pronounced, because the height of the peaks decreases more slowly than that for the flat region. The location of the peaks is in accordance with

the propagation speed,  $|v| = 1/\sqrt{2}$ , once we take in to account the fact that a single step of our walk is a product of two nearest neighbor operators,  $U_e$  and  $U_o$ .

- The size of the tail of the amplitude distribution is limited by  $(\epsilon t)^{-1} \sim t^{-1/3}$ , which gives  $\Delta n_{>} = \Delta(\epsilon t) = O(t^{1/3})$ . On the inner side, the width of the peaks is governed by  $|\omega_k'' t|^{-1/2} \sim t^{-1/3}$ . For  $|n| = (\sqrt{2} - \delta)t$ , this gives  $\Delta n_{<} = \Delta(\delta t) = O(t^{1/3})$ . The peaks therefore make a negligible contribution to the probability distribution,  $O(t^{-1/3})$ .

- Rapid oscillations contribute to the probability distribution (and hence to its moments) only at subleading order. They can be safely ignored in an asymptotic analysis, retaining only the smooth part of the probability distribution.

- The quantum random walk spreads linearly in time, with a speed smaller by a factor of  $\sqrt{2}$  compared to a directed walk. This speed is a measure of its mixing behavior and hitting probability. The probability distribution is qualitatively similar to a uniform distribution over the interval  $[-\sqrt{2}t, \sqrt{2}t]$ . In particular, the  $m^{\text{th}}$  moment of the probability distribution is proportional to  $t^m$ . This behaviour is in sharp contrast to that of the

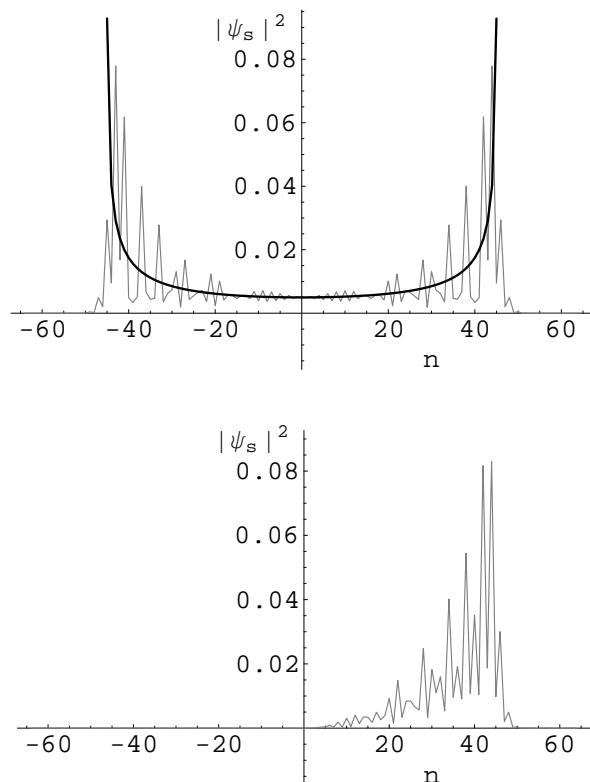


FIG. 2: Probability distribution after 32 time steps for the symmetric quantum random walk  $\psi_s$ . In the top figure, the dark curve denotes the smoothed distribution of Eq.(27). The bottom figure shows the distribution in the presence of an absorbing wall on the left side of  $n = 0$ .

classical random walk. The classical random walk produces a binomial probability distribution, which in the symmetric case has a single peak centered at the origin and variance proportional to  $t$ . The linear spread in time of our quantum random walk is achieved even when  $\psi$  has 50% probability to stay put at the same location at every step, as can be seen from Eqs.(15,16). This means that our walk is more directed and less of a zigzag.

- Above properties agree with those obtained in Refs.[9, 13] for a quantum random walk with a coin-toss instruction (extra factors of 2 appear in our results because of difference in our conventions), demonstrating that the coin offers no advantage in this particular set up. Essentially, we have absorbed the two states of the coin in to the even/odd site label at no extra cost. By making the coin states part of the position space, we have eliminated quantum entanglement between the coin and the position degrees of freedom completely—only superposition representing the amplitude distribution survives [14]. Such a reorganisation would be a tremendous advantage in any practical implementation of the quantum random walk, because quantum entanglement is highly fragile against environmental disturbances while mere superposition is much more stable. The cost for gaining this advantage is the loss of short distance homogeneity—translational invariance holds in steps of 2 instead of 1.

- Comparison of the numerically evaluated probability distributions in Fig.2, without and with the absorbing wall, shows that the absorbing wall disturbs the evolution of the walk only marginally. The probability distribution in the region close to  $n = 0$  is depleted as anticipated, while it is a bit of a surprise that the peak height near  $n = \sqrt{2}t$  increases slightly. As a result, the escape speed from the wall is little higher than the spreading speed without the wall. Overall, the part of the quantum random walk going away from the absorbing wall just takes off at a constant speed, hardly ever returning to the starting point. Again, this behavior is in a sharp contrast to that of the classical random walk, which always returns to the starting point, sooner or later. We also find that the first two time steps dominate absorption,  $P_{s,abs}(t = 1) = 0.25$  and  $P_{s,abs}(t = 2) = 0.375$ , with very little absorption later on. Asymptotically, the net absorption probability approaches  $P_{s,abs}(\infty) \approx 0.4098$  for the symmetric walk. This value is smaller than the corresponding result  $P_{abs}(\infty) = 2/\pi$  for the symmetric quantum random walk with a coin-toss instruction [13].

## IV. QUANTUM RANDOM WALK ON A HYPERCUBIC LATTICE

### A. 2-dim Lattice

Next let us consider the situation for  $d = 2$ . The partitioned free Hamiltonian is given by

$$H_o|x, y\rangle = -\frac{i}{2}\left[(-1)^x|x + (-1)^x, y\rangle\right.$$

$$\left. + (-1)^{x+y}|x, y + (-1)^y\rangle\right], \quad (31)$$

$$H_e|x, y\rangle = \frac{i}{2}\left[(-1)^x|x - (-1)^x, y\rangle\right.$$

$$\left. + (-1)^{x+y}|x, y - (-1)^y\rangle\right], \quad (32)$$

$$H|x, y\rangle = (H_o + H_e)|x, y\rangle$$

$$= -\frac{i}{2}\left[|x + 1, y\rangle - |x - 1, y\rangle\right.$$

$$\left. + (-1)^x(|x, y + 1\rangle - |x, y - 1\rangle)\right]. \quad (33)$$

More explicitly, the  $4 \times 4$  blocks of the Hamiltonian are:

$$H_o^B = -\frac{i}{2} \begin{pmatrix} 0 & -1 & -1 & 0 \\ 1 & 0 & 0 & 1 \\ 1 & 0 & 0 & -1 \\ 0 & -1 & 1 & 0 \end{pmatrix} \begin{matrix} 00 \\ 10 \\ 01 \\ 11 \end{matrix} \quad (34)$$

$$= -\frac{1}{2}(I \otimes \sigma_2 + \sigma_2 \otimes \sigma_3), \quad (35)$$

where the column on the right denotes the vertices of the elementary square on which  $H_o^B$  operates. Similarly,  $H_e^B = -H_o^B$ , when operating on the square with vertices  $\{00, -10, 0-1, -1-1\}$ . Noting that  $H_o^2 = H_e^2 = \frac{1}{2}I$ , the block-diagonal matrices are easily exponentiated to

$$U_{o(e)} = cI - is\sqrt{2}H_{o(e)}, \quad |c|^2 + |s|^2 = 1. \quad (36)$$

The parameter  $c$  (or  $s$ ) is to be tuned to achieve the fastest diffusion across the lattice.

The quantum random walk with the Dirac operator spreads on a two-dimensional grid as illustrated in Fig.3. The continuum Dirac Hamiltonian has exact rotational symmetry, and that survives to an extent even after discretisation on a hypercubic lattice. After a point start, the random walk spreads essentially isotropically at distances much larger than the lattice spacing, while the hypercubic symmetry governs the random walk pattern at shorter distances. Of course, the hypercubic symmetry would be exact for a  $d$ -dim random walk constructed as a tensor product of  $d$  one-dimensional random walks.

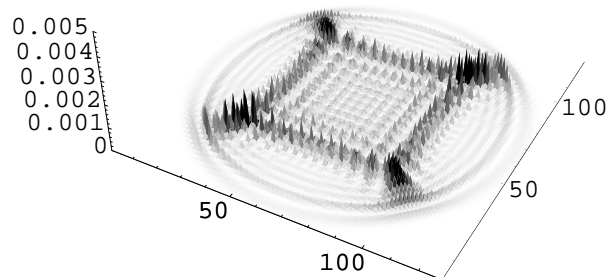


FIG. 3: Probability distribution for the quantum random walk on a two-dimensional  $128 \times 128$  grid after 61 time steps. A symmetric start, i.e.  $\psi(x, y, 0) = (\delta_{x0}\delta_{y0} + i\delta_{x1}\delta_{y1})/\sqrt{2}$ , was used. Darker shades on the grey-scale indicate larger probability.

### B. 3-dim Lattice

Next let us look at the situation for  $d = 3$ . The partitioned free Hamiltonian is given by

$$H_o|x, y, z\rangle = -\frac{i}{2} \left[ (-1)^x |x + (-1)^x, y, z\rangle + (-1)^{x+y} |x, y + (-1)^y, z\rangle + (-1)^{x+y+z} |x, y, z + (-1)^z\rangle \right], \quad (37)$$

$$H_e|x, y, z\rangle = \frac{i}{2} \left[ (-1)^x |x - (-1)^x, y, z\rangle + (-1)^{x+y} |x, y - (-1)^y, z\rangle + (-1)^{x+y+z} |x, y, z - (-1)^z\rangle \right], \quad (38)$$

$$H|x, y, z\rangle = (H_o + H_e)|x, y, z\rangle = -\frac{i}{2} \left[ |x + 1, y, z\rangle - |x - 1, y, z\rangle + (-1)^x (|x, y + 1, z\rangle - |x, y - 1, z\rangle) + (-1)^{x+y} (|x, y, z + 1\rangle - |x, y, z - 1\rangle) \right]. \quad (39)$$

More explicitly, the  $8 \times 8$  blocks of the Hamiltonian are:

$$H_o^B = -\frac{i}{2} \begin{pmatrix} 0 & -1 & -1 & 0 & -1 & 0 & 0 & 0 \\ 1 & 0 & 0 & 1 & 0 & 1 & 0 & 0 \\ 1 & 0 & 0 & -1 & 0 & 0 & 1 & 0 \\ 0 & -1 & 1 & 0 & 0 & 0 & 0 & -1 \\ 1 & 0 & 0 & 0 & 0 & -1 & -1 & 0 \\ 0 & -1 & 0 & 0 & 1 & 0 & 0 & 1 \\ 0 & 0 & -1 & 0 & 1 & 0 & 0 & -1 \\ 0 & 0 & 0 & 1 & 0 & -1 & 1 & 0 \end{pmatrix} \begin{matrix} 000 \\ 100 \\ 010 \\ 110 \\ 001 \\ 101 \\ 011 \\ 111 \end{matrix} \\ = -\frac{1}{2} (I \otimes I \otimes \sigma_2 + I \otimes \sigma_2 \otimes \sigma_3 + \sigma_2 \otimes \sigma_3 \otimes \sigma_3), \quad (40)$$

with the column on the right indicating the vertices of the elementary cube on which  $H_o^B$  operates. Likewise,  $H_e^B = -H_o^B$ , when operating on the elementary cube with vertices  $\{000, -100, 0-10, -1-10, 00-1, -10-1, 0-1-1, -1-1-1\}$ . With  $H_o^2 = H_e^2 = \frac{3}{4}I$ , the block-diagonal matrices exponentiate to

$$U_{o(e)} = cI - is \frac{2}{\sqrt{3}} H_{o(e)}, \quad |c|^2 + |s|^2 = 1. \quad (41)$$

Again  $c$  (or  $s$ ) is a parameter to be tuned to achieve the fastest diffusion across the lattice.

### C. $d$ -dim Lattice

We can now observe a pattern in the explicit results for  $d = 1, 2, 3$  above. The  $2^d \times 2^d$  blocks of the Hamiltonian can be written as sums of tensor products of Pauli matrices. As suggested by Eqs.(35,40),

$$H_o^B = -\frac{1}{2} \sum_{j=1}^d I^{\otimes(d-j)} \otimes \sigma_2 \otimes \sigma_3^{\otimes(j-1)}, \quad (42)$$

and  $H_e^B = -H_o^B$  when operating on the hypercube with coordinates flipped in sign. The block-diagonal matrices satisfy  $H_o^2 = H_e^2 = \frac{d}{4}I$ , and exponentiate to

$$U_{o(e)} = cI - is \frac{2}{\sqrt{d}} H_{o(e)}, \quad |c|^2 + |s|^2 = 1. \quad (43)$$

## V. SEARCH ON A HYPERCUBIC LATTICE USING THE DIRAC OPERATOR

### A. Strategy

A clear advantage of quantum random walks is their linear spread in time, compared to square-root spread in time for classical random walks. So they are expected to be useful in problems requiring fast hitting times. Several examples of this nature have been explored in graph theoretical and sampling problems (see Refs.[15, 16] for reviews). Here we consider the particular case of using the quantum random walk to find a marked vertex on a hypercubic lattice (see also Refs.[5, 6]).

Consider a  $d$ -dim hypercubic lattice with  $N = L^d$  vertices, one of which is marked. The quantum algorithmic strategy for the search process is to construct a Hamiltonian evolution, where the kinetic part of the Hamiltonian diffuses the amplitude distribution all over the lattice while the potential part of the Hamiltonian attracts the amplitude distribution towards the marked vertex [17]. The optimisation criterion is to concentrate the amplitude distribution towards the marked vertex as quickly as possible. In his algorithm, Grover constructed a global operator that allows diffusion from any vertex to any other vertex in just one step. Under different circumstances, when diffusion is restricted to be ultra-local (i.e. one can only go from a vertex to its neighbours in one step), one must find an appropriate diffusion operator that provides fast propagation of spatial modes. Obviously, the Dirac operator is better suited to this task than the Laplacian operator.

To search for a marked vertex, say the origin, we need to attract the quantum random walk towards it. This can be accomplished by adding a potential to the free Hamiltonian,

$$V = V_0 \delta_{\vec{x},0}. \quad (44)$$

Exponentiation of this potential produces a phase change for the amplitude at the marked vertex. It is optimal to choose the magnitude of the potential to make the phase maximally different from 1, i.e.  $e^{-iV_0\tau} = -1$ , whereby the phase becomes a reflection operator (binary oracle),

$$R = I - 2|\vec{0}\rangle\langle\vec{0}|. \quad (45)$$

The search algorithm alternates between the diffusion and the reflection operators, yielding the evolution

$$\psi(\vec{x}; t_1, t_2) = [W^{t_1} R]^{t_2} \psi(\vec{x}; 0, 0). \quad (46)$$

Here  $t_2$  is the number of oracle calls, and  $t_1$  is the number of random walk steps between the oracle calls. Both have to be optimised, in addition to  $c$  and depending on the size and dimensionality of the lattice, to find the quickest solution to the search problem.

Fastest search amounts to finding the shortest unitary evolution path between the initial state, typically chosen as the uniform superposition state  $|s\rangle = \sum_x |\bar{x}\rangle/\sqrt{N}$ , and the marked state  $|\bar{0}\rangle$ . This path is a circular arc (geodesic) from  $|s\rangle$  to  $|\bar{0}\rangle$ . With the random walk diffusion operator  $W$ , evolution of the state  $|\psi\rangle$  does not remain restricted to the two-dimensional subspace formed by  $|s\rangle$  and  $|\bar{0}\rangle$ . Thus to optimise our algorithm, we need to tune the parameters so as to

- (a) maximise the projection of the state  $|\psi\rangle$  on to the two-dimensional  $|s\rangle - |\bar{0}\rangle$  subspace, and
  - (b) maximise the angle of rotation by the operator  $W^{t_1}R$ , for the projected component of  $|\psi\rangle$  in the  $|s\rangle - |\bar{0}\rangle$  subspace.
- We have explored this optimisation numerically.

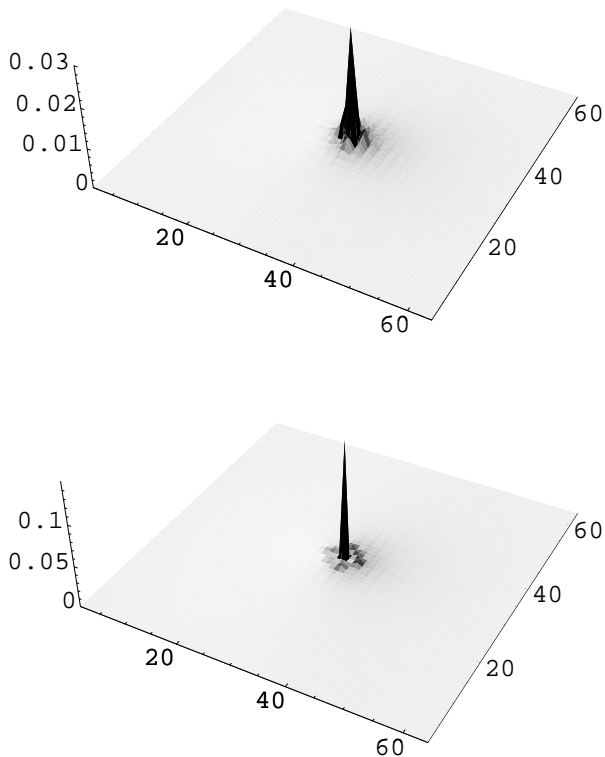


FIG. 4: Probability distribution for the quantum random walk search problem on a two-dimensional  $64 \times 64$  grid, at the instance when the probability at the marked vertex attains its largest value. The number of random walk steps are  $t_1 = 1$  (top) and  $t_1 = 3$  (bottom).

## B. Numerical Results

We carried out computer simulations of the quantum random walk search problem with a single marked vertex, for  $d = 2, 3$ . The algorithm was optimised by tuning the parameters  $c$  and  $t_1$ , so as to minimise the number of oracle calls  $t_2$  required to find the marked vertex. The following is a summary of our observations:

- An unbiased search starts with a uniform probability distribution over the whole lattice. Thereafter, the probability at the marked vertex goes through periodic cycles of rise and fall as a function of time step. It is crucial to stop the algorithm at the right instance to find the marked vertex with a significant probability.

- Our best results are obtained with  $c = 1/\sqrt{2}$  and  $t_1 = 3$ . In this case, the probability at the marked vertex reaches its largest value, and  $t_2$  achieves its smallest value. With these parameters, the probability at the marked vertex shows a periodic sinusoidal behaviour, which persists for more than 30 cycles without any visible deviation. Also, apart from the uniform background, the probability distribution shows a sharp single-point delta function at the marked vertex. These features indicate that the walk evolves largely in the two-dimensional subspace formed by the uniform state and the marked state.

- For  $c < 1/\sqrt{2}$ , the walk diffuses more slowly, and  $t_2$  increases. For  $c > 1/\sqrt{2}$ , the probability at the marked vertex loses its periodic sinusoidal behaviour, suggesting that the walk no longer remains confined to the two-dimensional subspace. For the optimal choice  $c = 1/\sqrt{2}$ , the probability of the walk remaining at the same vertex equals that for moving to a neighbouring vertex, which corresponds to the most efficient mixing between odd and even sublattices.

- For  $t_1 < 3$ , the probability distribution spreads out instead of being a delta function at the marked vertex, as illustrated in Fig.3. This decreases the peak probability at the marked vertex. Moreover,  $t_2$  increases. For  $t_1 > 3$ , the probability at the marked vertex loses its sinusoidal behaviour, again with a decrease in the peak probability. In both cases, the changes indicate that the walk is drifting out of the two-dimensional subspace. An appropriate choice of  $t_1$  is thus crucial to keep the walk close to the two-dimensional subspace.

- For the 2-dim walk, the largest probability at the marked vertex is predicted to be  $O(1/\log N)$ , which occurs after  $O(\sqrt{N \log N})$  time steps [5, 6]. To make the marked vertex probability  $O(1)$ , an amplitude amplification procedure is required [18], and the overall search algorithm scales as  $O(\sqrt{N \log N})$ . Our numerical results, shown in Fig.5, are consistent with these expectations. Simple fits provide the parametrisations:

$$\begin{aligned} O(1/\log N) &\longrightarrow 2.12/\log_2 N, \\ O(\sqrt{N \log N}) &\longrightarrow 0.137\sqrt{N \log_2 N}. \end{aligned} \quad (47)$$

- For the walk in more than two dimensions, the largest probability at the marked vertex is predicted to be  $O(1)$ ,

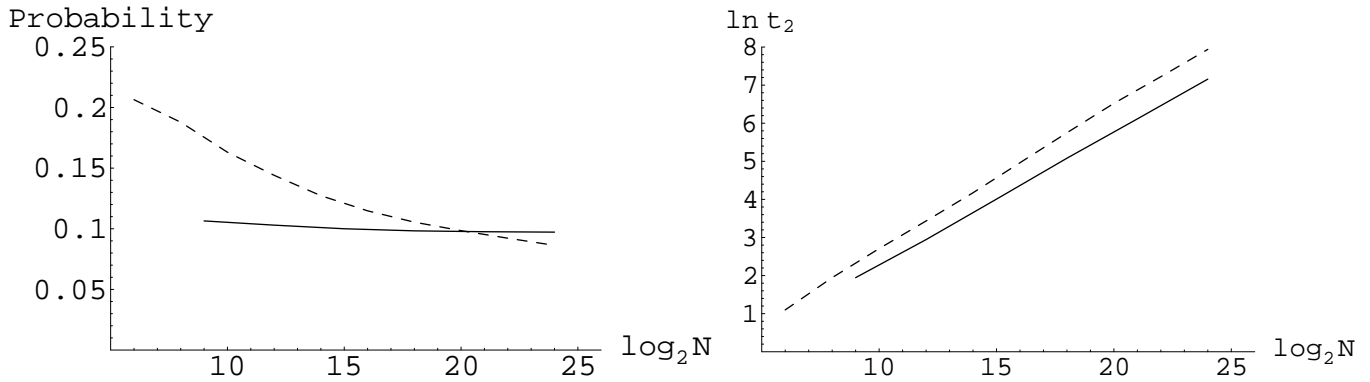


FIG. 5: The peak probability at the marked vertex for the quantum random walk search problem (left), and the number of time steps required to reach it (right), as a function of the database size. The dashed and continuous curves correspond to  $d = 2$  and  $d = 3$  respectively.  $c = 1/\sqrt{2}$  and  $t_1 = 3$  were used, with  $N$  ranging from  $2^6$  to  $2^{24}$ .

which occurs after  $O(\sqrt{N})$  time steps [5, 6]. Our numerical results for the 3-dim walk, also displayed in Fig.5, agree with these scaling rules. Simple fits provide the parametrisations:

$$O(1) \longrightarrow 0.0969, \quad O(\sqrt{N}) \longrightarrow 0.313\sqrt{N}. \quad (48)$$

These results demonstrate that our quantum random

walk algorithm achieves the optimal scaling behaviour for the problem of finding a marked vertex on a hypercubic lattice. Thus our quantum random walk, based on the Dirac operator and not containing a coin toss instruction, is no less effective in its diffusion properties than the earlier quantum random walks that use a coin toss instruction.

- 
- [1] R. Motwani and P. Raghavan, *Randomized Algorithms*, (Cambridge University Press, Cambridge, 1995).
- [2] A. Patel, K.S. Raghunathan and P. Rungta, Phys. Rev. A71 (2005) 032347, e-print quant-ph/0405128.
- [3] A. Patel and K.S. Raghunathan, in preparation.
- [4] In general, energy includes a mass term. The mass operator behaves like the  $\vec{k} = 0$  mode, and changes the phase of the quantum amplitude. But it does not contribute to diffusion, and so we leave the mass term out.
- [5] A. Ambainis, J. Kempe and A. Rivosh, Proceedings of ACM-SIAM SODA'05 (ACM Press, New York, 2005), to appear, e-print quant-ph/0402107.
- [6] A.M. Childs and J. Goldstone, Phys. Rev. A 70 (2004) 042312, e-print quant-ph/0405120.
- [7] L. Susskind, Phys. Rev. D 16 (1977) 3031.
- [8] This is in spite of the fact that Dirac spinors require more than two components for  $d > 2$ . For example, in 3-dimensions, a Rubik's cube can have the central cube labeled "o" and the eight corner cubes labeled "e".
- [9] A. Nayak and A. Vishwanath, DIMACS Technical Report 2000-43, e-print quant-ph/0010117.
- [10] J.L. Richardson, Comput. Phys. Commun. 63 (1991) 84.
- [11] D.A. Meyer, J. Stat. Phys. 85 (1996) 551.
- [12] This transformation is a phase-shift of  $\pi/2$  in momentum space. It changes  $\cos(k)$  terms associated with second derivatives to  $\sin(k)$  terms associated with first derivatives.
- [13] A. Ambainis, E. Bach, A. Nayak, A. Vishwanath and J. Watrous, Proceedings of STOC'01 (ACM Press, New York, 2001), p.37.
- [14] Entanglement is always defined with respect to a specific division of the whole system in to its parts. If the division scheme is altered, entanglement can change.
- [15] J. Kempe, Contemp. Phys. 44 (2003) 307, e-print quant-ph/0303081.
- [16] A. Ambainis, Int. J. Quantum Inf. 1 (2003) 507, e-print quant-ph/0403120.
- [17] L.K. Grover, Pramana 56 (2001) 333, quant-ph/0109116.
- [18] G. Brassard, P. Hoyer, M. Mosca and A. Tapp, in *Quantum Computation and Information*, AMS Contemporary Mathematics Series Vol. 305, eds. S.J. Lomonaco and H.E. Brandt (AMS, Providence, 2002), quant-ph/0005055.